Site NGHP-01-02

By T. Collett, M. Riedel, J. Cochran, R. Boswell, J. Presley, P. Kumar, A. Sathe,
A. Sethi, M. Lall, and the National Gas Hydrate Program Expedition 01 Scientists

Scientific Investigations Report 2012–5054

U.S. Department of the Interior
U.S. Geological Survey

Contents

Figures

Site NGHP-01-02

By T. Collett, M. Riedel, J. Cochran, R. Boswell, J. Presley, P. Kumar, A. Sathe, A. Sethi, M. Lall, and the National Gas Hydrate Program Expedition 01 Scientists

Background and Objectives

Site NGHP-01-02 (Prospectus Site KGGH03-A) is located at 15° 52.119'N, 081° 49.3583'E in the Krishna-Godavari (KG) Basin (fig. 1). The water depth is ~1,058 m. This site was not selected as a primary coring site and only LWD/MWD data were recovered.

The objectives of the work carried out at this site follow the general objectives of NGHP Expedition 01, but focus on the LWD/MWD operations only:

- Study the occurrence of gas hydrate and establish the background geophysical baselines for gas-hydrate studies;
- Define the relationship between the sedimentology and structure of the sediments and the occurrence and concentration of gas hydrate;
- Calibrate remote sensing data such as seismic data by acquiring LWD/MWD; and
- Comparison to LWD data acquired in nearby industry well GD-3-1.

Site NGHP-01-02 is located along seismic line AD-94-13 (NW-SE oriented). The area is characterized by a ridge with steeply dipping stratigraphy and gas-related increases in seismic amplitudes ("brightening"; fig. 2). The site was originally proposed about 1,600 m further upslope to the NW (location KGGH03) but was subsequently moved to enable data acquisition within the large-amplitude, steeply dipping reflectors within the gas-hydrate stability field near the crest of the ridge structure.

A bottom-simulating reflector (BSR) is seen along the line, especially between shot points 190 and 260 (fig. 3). The depth of the BSR is estimated at ~170 mbsf based on 0.216 s TWT and a velocity of 1,580 m/s. Operations at this site were limited to a maximum depth of 250 MBSF to avoid drilling into the deeper high-amplitude reflectors.

Operations

This operations summary covers the Chennai port call at the beginning of Leg 2, the transit to Site NGHP-01-02 (KGGH03-A), and LWD/MWD drilling operations in Holes NGHP-01-02A and NGHP-01-02B (fig. 4). Schedule details and statistics for this site can be found as Appendixes:

- Appendix 1: NGHP Expedition 01 Operations Schedules
- Appendix 2: NGHP Expedition 01 Operations Statistics

Included in the "Methods" section is a list of standard or commonly used operations terms and acronyms.

Hole NGHP-01-02A

Leg 2 of the five-leg NGHP Expedition 01 began after completing a 3.3 day port call in Chennai. This was the first Chennai port call and was primarily used for changing out the scientific staff compliment, loading all Schlumberger LWD/MWD equipment and engineers, and taking on general supplies. The drilling contractor did not change out crews during this port call. The vessel departed Chennai with the last line away from Harbor Basin West Quay 4 (passenger terminal) at 1320 hr May 19, 2006. The 191.0 NMI transit was made to Site NGHP-01-02 (KGGH03-A) at an average speed of 10.4 knots.

Hole NGHP-01-02A was drilled to provide a shallow test hole for the LWD/MWD tools and was the first hole of what was to become a 12-hole LWD/MWD transect. The vessel was switched from cruise mode to DP control at 0740 hr May 20, 2006 and a positioning beacon was deployed at the Hole NGHP-01-02A location coordinates. The LWD/MWD tools, consisting of the GeoVISION (RAB), EcoScope, SonicVISION, TeleScope, and ProVISION (NMR), were assembled. One and one-half hours were spent troubleshooting the NMR tool before the decision was made to move ahead with the deployment. The nuclear source was loaded, and the drill string was lowered to a depth of 150.0 mbrf. Two additional hours were then spent testing the tools and troubleshooting the telemetry system. The Minitron was turned on and the pipe trip continued to ~30 m off the sea floor. There, the tool's on/off pumping rates were calibrated and pumping rates were refined to reduce noise in the telemetry data. The drill string was spaced out for spudding and a tag of the sea floor indicated a mudline depth of 1,069.0 mbrf. For reference, the PDR depth at this site, adjusted to the rig floor DES, was 1,069.0 mbrf. Hole NGHP-01-02A was spudded at 2355 hr on May 20. LWD/MWD drilling continued at a controlled rate of 18.3 m/h (average net ROP including

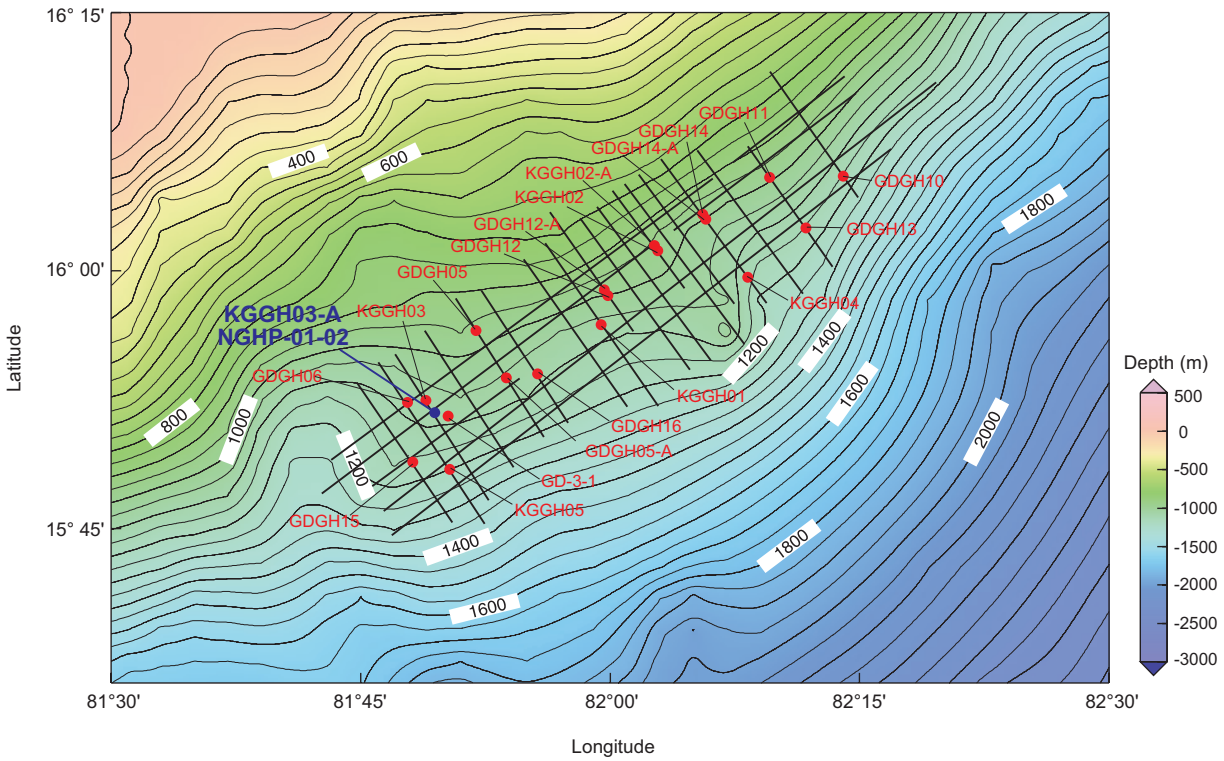

Figure 1. Location of Site NGHP-01-02 (Prospectus Site KGGH03-A) in the Krishna-Godavari (KG) Basin.

connection time) to a total depth of 50.3 mbsf. The drill string was pulled clear of the sea floor at 0305 hr ending Hole NGHP-01-02A and beginning Hole NGHP-01-02B.

Hole NGHP-01-02B

The vessel was offset 3 m to the north of Hole NGHP-01-02A and Hole NGHP-01-02B was spudded at 0325 hr May 21, 2006. LWD/MWD drilling continued at a controlled rate of 16.1 m/h (average net ROP including connection time) to a total depth of 250.0 mbsf. The hole was displaced with 60 barrels of 10.5 ppg mud and the drill string was recovered with the top drive to a depth of 76.3 mbsf. There the hole was reverse logged back to the sea floor. The drill string was pulled clear of the sea floor at 2215 hr and by 0030 hr May 22, 2006 the drill string was recovered to the BHA. The drill collars were racked back in the derrick, the NMR tool was laid out, the nuclear source was removed, and data was downloaded. By 0315 hr the rig was secured for transit and got underway for Site NGHP-01-03 (GDDH05-A). This ended operations at Site NGHP-01-02.

Downhole Logging

Logging While Drilling

Operations

LWD operations at Site NGHP-01-02 included two holes: a shallow hole (NGHP-01-02A) drilled to 50 mbsf and a deep hole (NGHP-01-02B) drilled to 250 mbsf. LWD tools in the BHA included the GeoVISION resistivity, the EcoScope, the SonicVISION, the TeleScope MW, and the ProVISION NMR (the ProVISION, however, malfunctioned and did not record any data). For details on each LWD tool and the measurements it makes, see the "Downhole Logging" section in the "Methods" chapter.

After tagging the seafloor at 1,069 mbrf (driller's depth), Hole NGHP-01-02A was spudded at 2355 hr on May 20, 2006. To ensure that the LWD tools were powered up to measure real-time data for gas monitoring (see below), it was decided to drill from the beginning with the pumping rate at a relatively high value of 350–400 gpm. Although it was recognized that such a high pumping rate was likely to wash out

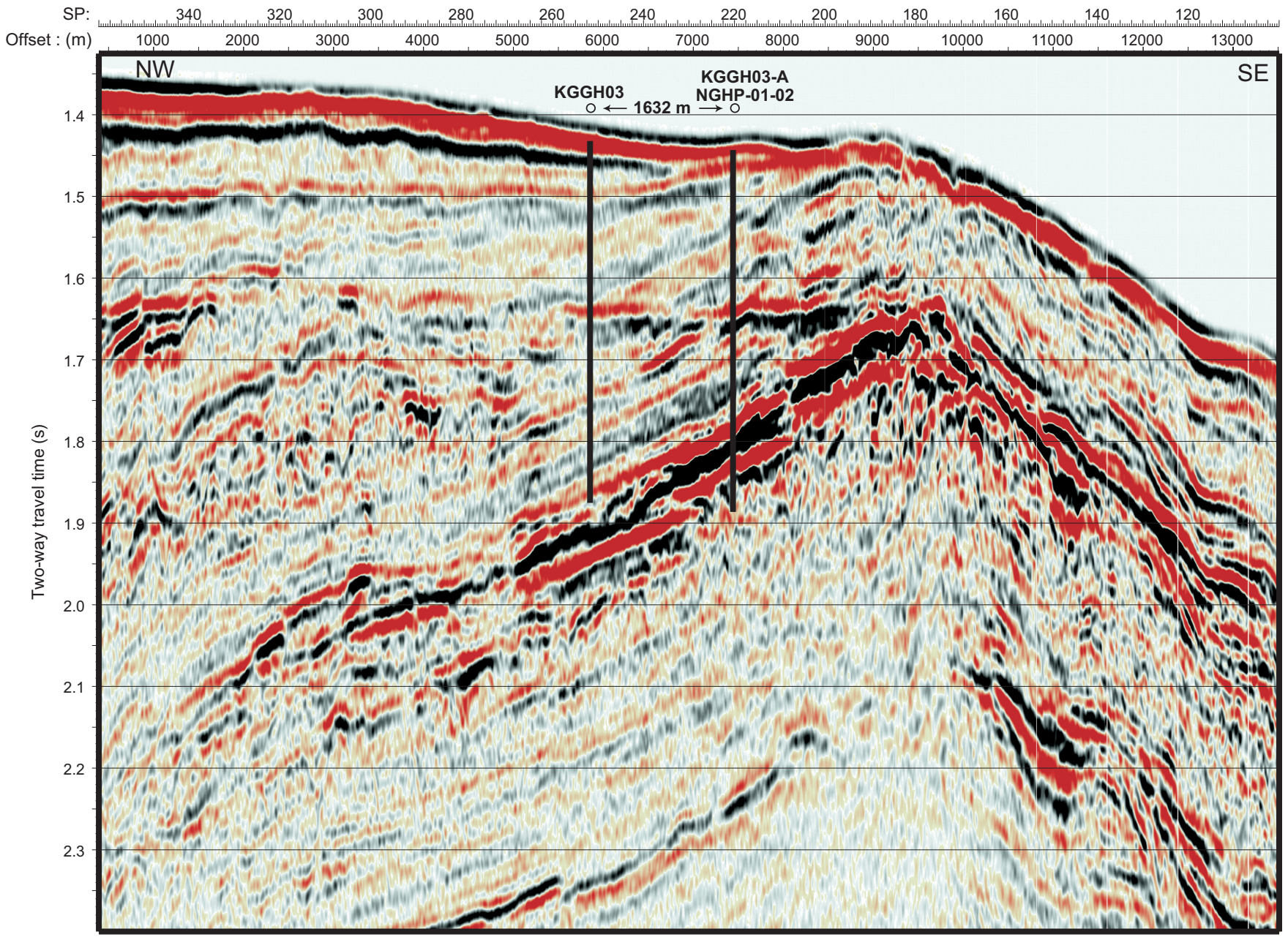

Figure 2. Section of 2D seismic line AD-94-13 around Site NGHP-01-02 (Prospectus Site KGGH03-A) showing overall structure of the setting and regional BSR occurrence. [BSR, bottom-simulating reflector]

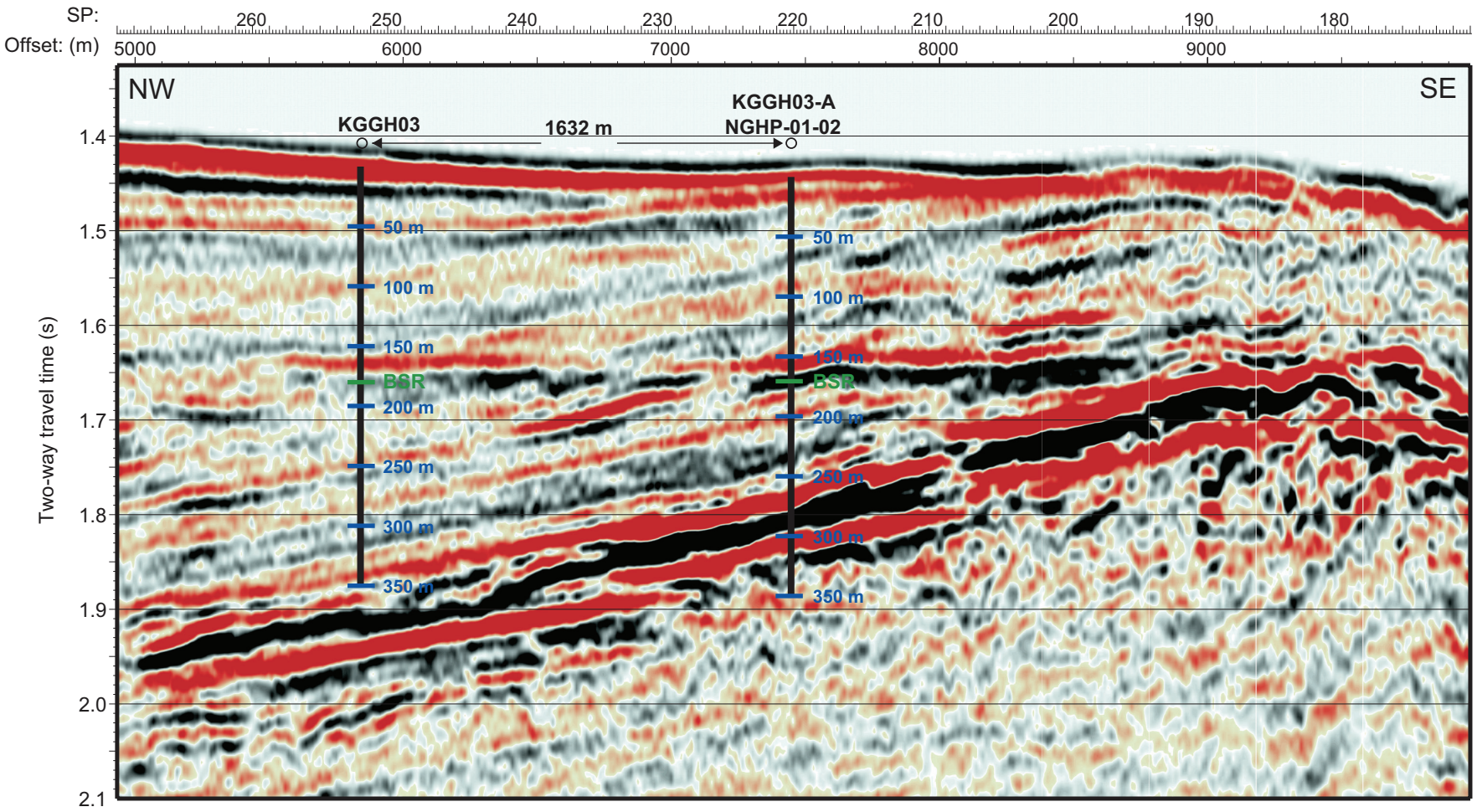

Figure 3. Section of seismic line AD-94-13 around Site NGHP-01-02 (Prospectus Site KGGH03-A) showing predicted formation tops and BSR depth (170 mbsf) based on a uniform seismic velocity of 1,580 m/s. [BSR, bottom-simulating reflector; mbsf, meters below sea floor; m/s, meters per second]

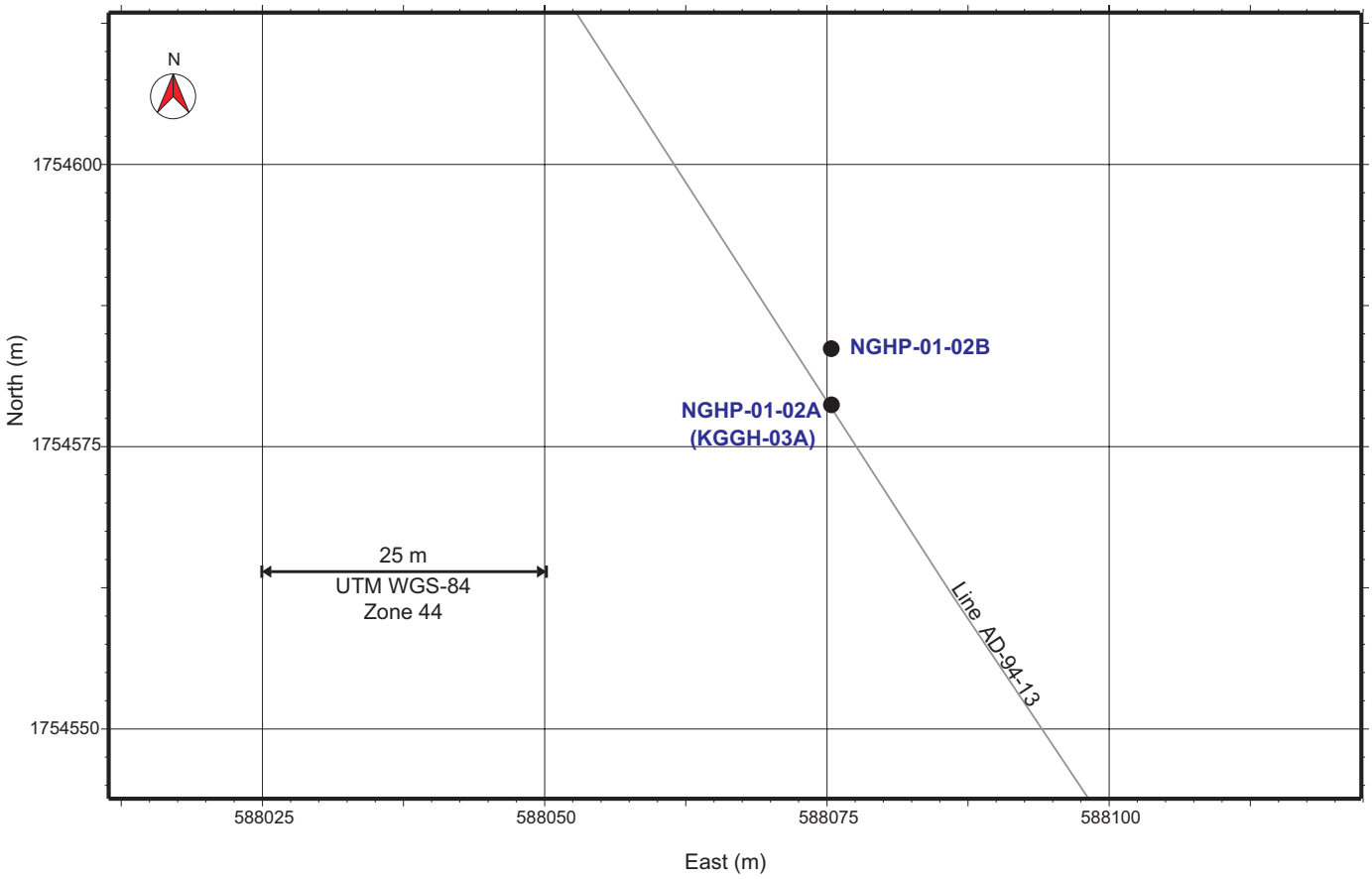

Figure 4. Map showing all holes occupied at Site NGHP-01-02 (KGGH03-A).

the hole near the seafloor, obtaining all the data needed for gas monitoring from the very start received higher priority in this first hole. The first 10 m of Hole NGHP-01-02A were drilled with a rotation rate of 10 rpm and a rate of penetration (ROP) of 25 m/h. Rotation rate was then increased to 30 rpm while keeping other parameters unchanged until 40 mbsf, and then proceeded to 60 rpm, keeping the instantaneous ROP around 25 m/h with depth. The target depth of 50 mbsf (1,116 mbrf) was reached at 0245 hr on May 21.

After pulling out of the completed hole just clear of the seafloor, the ship was moved by 3 m and Hole NGHP-01-02B was spudded at 0326 hr on May 21. To avoid washing out the hole near the seafloor, Hole NGHP-01-02B was spudded at a relatively low flow rate. The first 10 m were drilled at 50 gpm with a rotation rate of 10 rpm and a ROP of 25 m/h. Below 10 mbsf, the rotation rate was increased to 30 rpm and the flow rate to 100 gpm; over the range of 30–35 mbsf, the rotation rate was increased to 60 rpm and the flow rate was increased until the LWD tools turned on (350–400 gpm), continuing to drill with a ROP of 25 m/h. The target depth of 250 mbsf (1,316 mbrf) was reached at 1858 hr on May 21. While pulling out of hole, we logged the top 75 m to measure a caliper log in Hole NGHP-01-02B and compare it to the caliper in Hole NGHP-01-02A (which was spudded at a high pumping rate). Rig down and data download was completed at 0304 hr on May 22. (The depths in mbsf mentioned above are referenced to the seafloor depth tagged by the driller.)

Gas Monitoring with Real Time LWD/MWD Data

The LWD logs were acquired in the first holes drilled at Site NGHP-01-02 to plan coring and pressure coring operations in subsequent holes. As Holes NGHP-01-02A and NGHP-01-02B were drilled without coring, the LWD data had to be monitored for safety to detect gas entering the wellbore. As explained in the "Downhole logging" section of the "Methods" chapter, the primary measurement used for gas monitoring was the "annular pressure while drilling" (APWD) measured by the EcoScope tool in the borehole annulus. We looked for sudden decreases of more than 100 psi in the annular pressure, which could be due to low-density gas entering the wellbore. We also monitored pressure increases of the same magnitude, which could be due to fluid acceleration caused by a gas kick (Aldred and others, 1998).

Figure 5 shows the measured borehole fluid pressure profile in Hole NGHP-01-02B after subtraction of the hydrostatic pressure trend. This residual pressure curve shows only minor fluctuations, and the largest anomaly is a small positive step (about 15 psi) around 220 mbsf, which is well below the 100 psi level that would have required preventive action. Coherence of the sonic waveforms acquired by the SonicVISION tool was also monitored, focusing on the sound velocity in the borehole fluid. Gas indicators are loss of coherence in the waveforms and a slower sound velocity for the drilling fluid. No significant decrease of sonic waveform coherence throughout the interval drilled was found.

LWD Log Quality

Figure 5 also shows the quality control logs for Hole NGHP-01-02B. The two curves for rate of penetration (ROP) are an instantaneous rate of penetration (ROP_RM) and a rate of penetration averaged over 5 feet (ROP5_RM). The occasional large peaks in the instantaneous rate of penetration are artifacts due to depth fluctuations during pipe connections. The average ROP is about 20 m/h, which is sufficient to record high-resolution GeoVISION resistivity images (for details, see "Downhole Logging" in the "Methods" chapter).

The density (DCAV) and ultrasonic caliper logs (UCAV) show an average borehole diameter that is around 11 in at 26 mbsf and decreases to about 10 in below 145 mbsf. The bit size is 9 7/8 in, and most of the borehole below 145 mbsf is in gauge. The density correction, calculated from the difference between the short-and long-spaced density measurements, is everywhere within the interval 0–0.2 g/cm^3 (fig. 5), suggesting that the density measurements should be of good quality.

The same logs recorded in Hole NGHP-01-02A are shown for comparison (dashed curves). As this hole was mostly drilled to test and calibrate communication with the tools, it was drilled with a high pumping rate of ~400 gpm, and the calipers show a very enlarged hole resulting from this excessive pumping rate. As a result, data quality should be reduced in this hole, but the density correction does not indicate any significant adjustment.

Figure 6 is a summary of the LWD gamma ray, density, neutron porosity, and resistivity logs measured in Hole NGHP-01-02B. (SonicVISION results are not shown because they need processing on shore.) The same data from Hole NGHP-01-02A are shown as dashed lines in the same figure. Because of the very high flow rates used during their acquisition, these data are mostly shown for comparison. The gamma ray and resistivity logs measured by the GeoVISION and EcoScope LWD tools generally agree. The GeoVISION and EcoScope gamma ray curves have the same shape, but are offset by about 20–30 gAPI; this difference is most likely due to tool calibration. LWD gamma ray tools are calibrated with a total gamma ray standard that has a defined relative proportion of the radioactive elements (K, Th, and U). If this relative proportion in the formation were different from the standard, the tool calibration would not be entirely accurate.

The agreement between the resistivity curves is reassuring, because these resistivity measurements are based on different physical principles. The GeoVISION obtains resistivity by measuring current for a given voltage as in Ohm's law, and uses a low-frequency 1.5 kHz alternating current. The EcoScope tool instead measures resistivity from the attenuation and phase shift of 400 kHz and 2 MHz electromagnetic waves propagating through the formation (for more details, see the "Downhole logging" section in the "Methods" chapter). Figure 7 shows a comparison of the ring resistivity measured by GeoVISION with the attenuation and phase resistivity curves obtained by the EcoScope tool at different frequencies and coil spacings.

Figure 6 also shows two bulk density curves: RHOB is the average density obtained by the EcoScope tool while rotating, while IDRO (image-derived density) is the value of density measured when the sensors were in closest contact with the formation. The two density curves are very close except at depths less than 55 mbrf, where the caliper logs show the largest hole irregularities (fig. 5). The relatively poor hole quality may have degraded the density measurements in this shallow interval.

The BSR that should mark the bottom of the gas hydrate stability zone was estimated to be at a depth of 170 mbsf in this hole. The only change in the LWD logs near this depth is a small step-like decrease in resistivity (by ~0.7 Wm) at 159 mbsf (fig. 6).

The depths relative to seafloor were fixed for all of the LWD logs by identifying the step change in the GeoVISION gamma ray log at the seafloor. For Hole NGHP-01-02B, the gamma ray logging pick for the seafloor was at a depth of 1,064 mbrf, 5 m above the initial depth estimated by the drillers (1,069 mbrf). The rig floor logging datum was located 10.5 m above sea level.

LWD Porosities

Sediment porosities can be determined from analyses of recovered cores and from downhole measurements (see "Physical properties" and "Downhole logging" in the "Methods" chapter). Sediment porosities were calculated from the LWD density and neutron logs in Hole NGHP-01-02B. The LWD log-derived density measurements from Hole NGHP-01-02B were used to calculate sediment porosities (ϕ) using the standard density-porosity relation: $\phi = (r_g - r_b) / (r_g - r_w)$. We used a constant water density (r_w) equal to 1.03 g/cm^3 and a grain/matrix density (r_g) equal to 2.75 g/cm^3. The density log-derived porosities from Hole NGHP-01-02B range from about 60 percent at 30 mbsf to about 50 percent at 245 mbsf (fig. 6). The density porosities

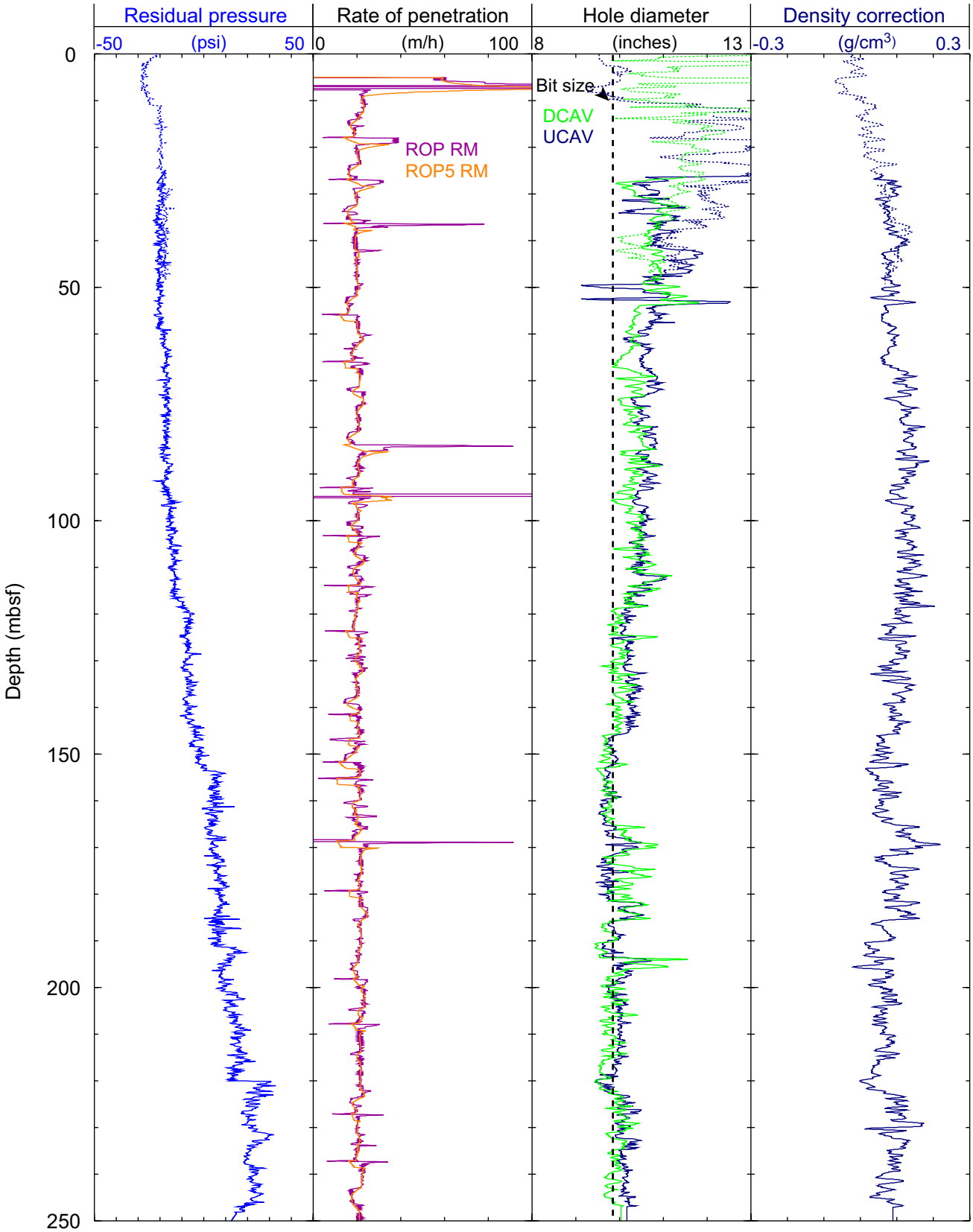

Figure 5. Monitoring and quality control LWD/MWD logs from Hole NGHP-01-02B. The same data recorded in Hole NGHP-1-02A are shown as dashed lines for comparison. [LWD/MWD, logging-while-drilling/measurement-while-drilling; ROP, Rate of penetration; ROP_RM, Instantaneous rate of penetration; ROP5_RM, Rate of penetration averaged over a 5-ft interval; UCAV, Ultrasonic caliper; DCAV, Density caliper]

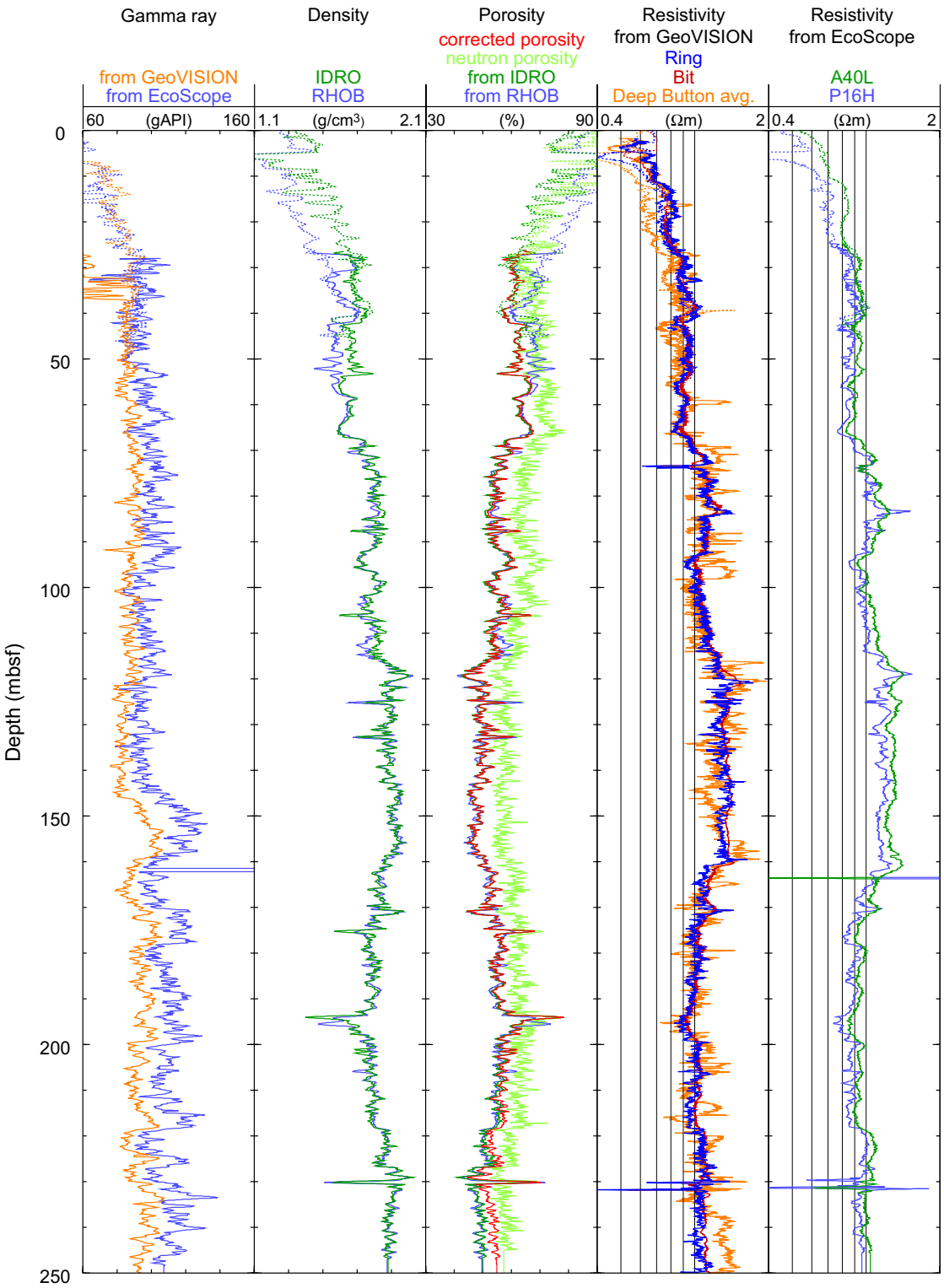

Figure 6. Summary of LWD log data from Holes NGHP-01-02A and NGHP-01-02B. Because of the very high flow rates used during their acquisition, the data from Hole NGHP-01-02A (dashed lines) are mostly shown for comparison. [LWD, logging-while-drilling; gAPI, American Petroleum Institute gamma ray units; IDRO, Image-derived density (EcoScope); RHOB, Bulk density (EcoScope); neutron, Thermal neutron porosity (EcoScope); corrected porosity, density porosity with core derived grain densities (EcoScope); RING, Ring resistivity (GeoVISION); BIT, Bit resistivity (GeoVISION); Deep Button avg., Button deep resistivity (GeoVISION); A40L, Attenuation resistivity measured at 400 kHz and a transmitter-receiver spacing of 40 in (EcoScope); P16H, Phase-shift resistivity at 2 MHZ and a transmitter-receiver spacing of 16 in (EcoScope)]

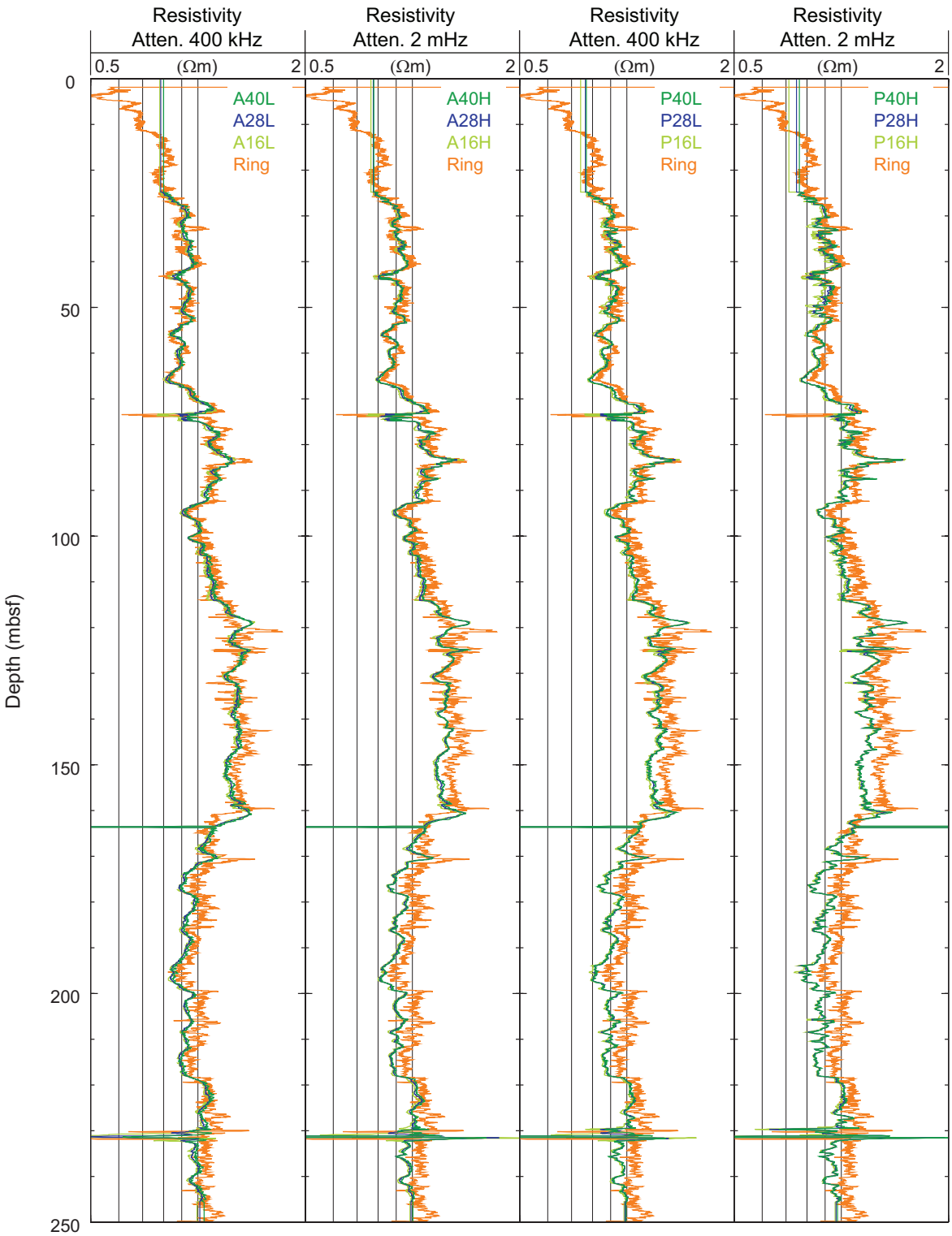

Figure 7. Comparison of LWD resistivity curves from Hole NGHP-01-02B with the attenuation and phase resistivity curves obtained by the EcoScope tool at different frequencies and coil spacings. [LWD, losing-while-drilling; Ring, Ring resistivity (GeoVISION); AXXL, Attenuation resistivity measured at a frequency of 400 kHz where XX is the transmitter-receiver spacing in inches (EcoScope); AXXH, Attenuation resistivity measured at a frequency of 2 MHz where XX is the transmitter-receiver spacing in inches (EcoScope); PXXL, Phase-shift resistivity measured at a frequency of 400 kHz where XX is the transmitter-receiver spacing in inches (EcoScope); PXXH, Phase-shift resistivity measured at a frequency of 2 MHz where XX is the transmitter-receiver spacing in inches (EcoScope)]

in figure 6 were calculated from both the bulk density (RHOB) and the image-derived density curve (IDRO). The two density porosities generally agree except at depths less than 55 mbrf, where the density measurements may have been affected by hole irregularity (see above). In this interval, the porosity computed from the bulk density seems unrealistically high and the image-derived density gives a more reasonable value around 60 percent.

In order to estimate the influence of variable grain density without any core sample measurements available at this site, we have calculated a 'corrected porosity' from the IDRO density log and from a least square third order polynomial fit with depth of the grain density measurements made on samples from nearby Sites NGHP-01-10 and NGHP-01-12. Except for the deepest part, the results show only little difference from the original density porosity derived with constant grain density.

The LWD neutron porosity log from Hole NGHP-01-02B (fig. 6) yielded sediment porosities ranging from an average value near the seafloor of about 65 percent at 30 mbsf to about 55 percent at 245 mbsf. Porosities measured by the neutron log are expected to be higher than those computed from the density log in clay-rich sediments, because the neutron log essentially quantifies hydrogen abundance, and counts hydrogen in clay minerals as porosity. The neutron porosity measured by the EcoScope tool shown in figure 6 is the "best thermal neutron porosity" (BPHI); it has been corrected so that the effect of clay should be reduced (Adolph and others, 2005). Despite this correction, it is consistently and uniformly higher than the density porosity.

LWD Borehole Images

The GeoVISION and EcoScope LWD tools generate high-resolution images of borehole log data. The EcoScope tool produces images of density and hole radius (computed on the basis of the density correction, which depends on the borehole standoff). The GeoVISION produces a gamma ray image and shallow, medium, and deep depth of investigation resistivity images.

Figure 8 shows some of the LWD images collected by the EcoScope and GeoVISION tools. It should be noted that the display in figure 8 is highly compressed in the vertical direction. The unwrapped images are about 80 cm wide (for a 10 in diameter borehole) and the vertical scale is compressed relative to the horizontal by a factor of about 55:1. These high-resolution images can be used for detailed sedimentological and structural interpretations and to image gas hydrate distribution in sediments (for example, in layers, nodules, fractures). Gas-hydrate-bearing sediments exhibit "bright" high resistivities within intervals of uniform or low bulk density. Layers with high resistivities and high densities are likely to be low porosity, compacted, or carbonate-rich sediments.

The two resistivity images in figure 8 correspond to two depths of investigation (for details, see "Downhole logging" in the "Methods" chapter). There is a general correlation between the resistivity and the density images, with high resistivity layers corresponding to relatively high densities. The density image shows a dark band with a clear sinusoidal shape around 193 mbsf, corresponding to a hole enlargement (11–12 in; see the caliper logs in fig. 5). The resistivity images show a variable resistivity interval at 192–194 mbsf. This feature may be a steeply dipping fault or fracture.

Gas Hydrate and Free Gas Occurrence

As previously discussed (see "Downhole Logging" in the "Methods" chapter), the presence of gas hydrate is generally characterized by increases in electrical resistivity and acoustic velocity that are not accompanied by a corresponding porosity decrease. A decrease in porosity alone in water-saturated sediments can result in an increase in resistivity and acoustic velocity. Resistivities logged in Hole NGHP-01-02B show a general negative correlation with porosity (fig. 6), suggesting that little or no gas hydrates are present.

To make a quantitative estimate of the amount of gas hydrate at Site NGHP-01-02, we followed the procedure described in "Downhole Logging" in the "Methods" chapter, to apply the Archie relationship to the resistivity and porosity logs recorded in Hole NGHP-01-02B.

The procedure and the results are shown in figure 9. The pore fluid resistivity (R_w) was estimated from Fofonoff (1985) using a linear temperature profile derived from the *in situ* temperature measurements at nearby Site NGHP-01-10 (6.5 °C at the seafloor; gradient of 45 °C/km, see "Downhole temperature measurements" in "Sites NGHP-01-10, 12, and 13") and a water salinity defined by the least square linear fit with depth of the values measured on pore water samples from Sites NGHP-01-10 and NGHP-01-12 (see "Downhole temperature measurements" in "Sites NGHP-01-10, 12, and 13"). The estimated m curve is derived from R_w, the porosity (ϕ) and resistivity (R_t) logs ($m_{est} = -\log F / \log\phi$, where $F = R_t / R_w$). As this relationship is defined for water-saturated sediments, the chosen value of $m = 2.1$ is given by the baseline of this curve in the low-resistivity intervals where there is likely no gas hydrate. Using the porosity log and Archie's equation ($R_0 = (a\, R_w) / \phi^m$), we derived the predicted resistivity of the water-saturated formation R_o. A qualitative influence of gas hydrate on the resistivity log is indicated by the difference between the R_0 and the measured resistivity R_t. The estimated water saturation, assumed to be the numerical complement of the hydrate saturation, is $S_w = (R_0/R_t)^{1/n}$, where

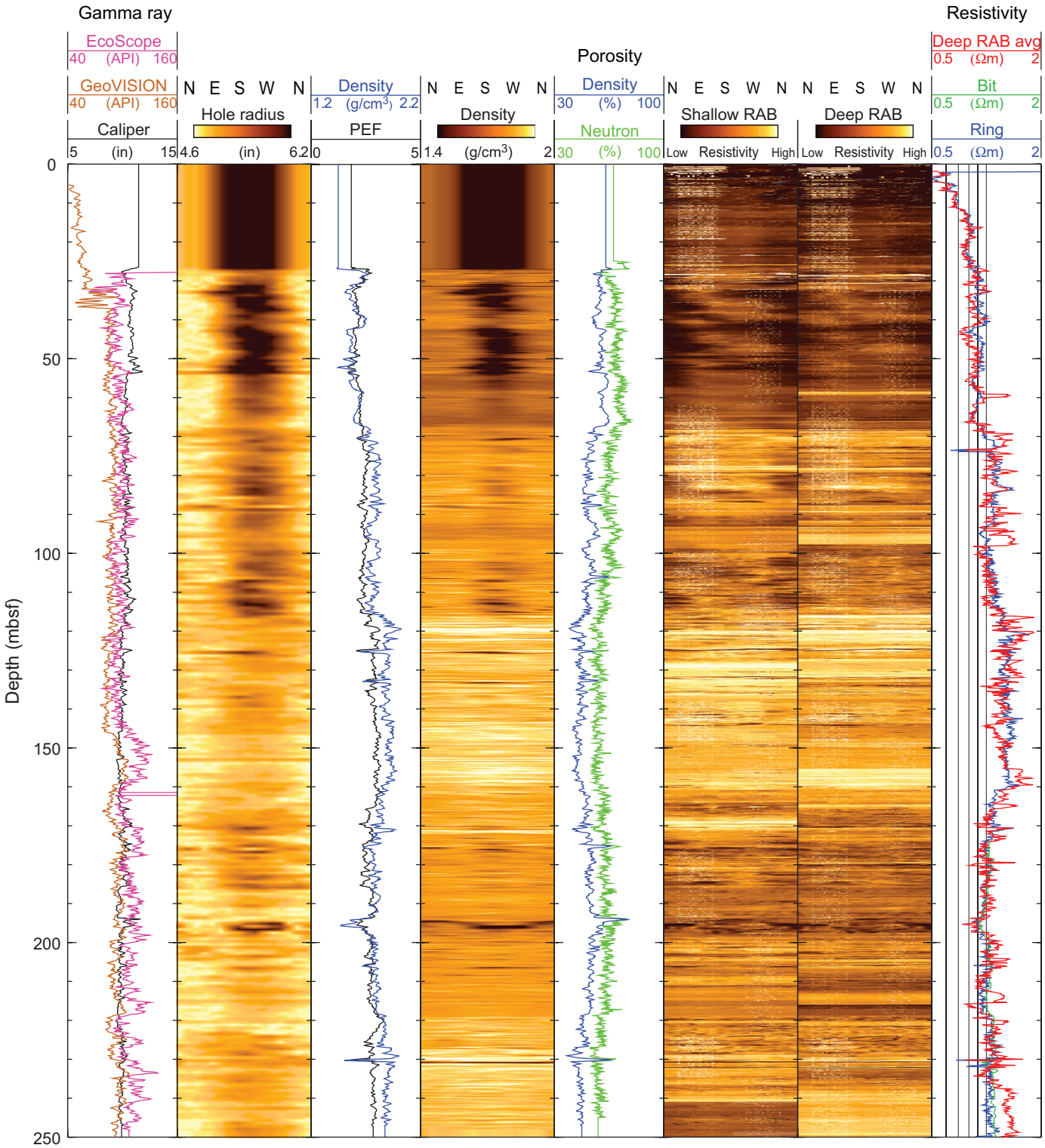

Figure 8. LWD image data from Hole NGHP-01-02B. [LWD, logging-while-drilling; gAPI, American Petroleum Institute gamma ray units; RAB, Resistivity-At-Bit image obtained by the GeoVISION tool]

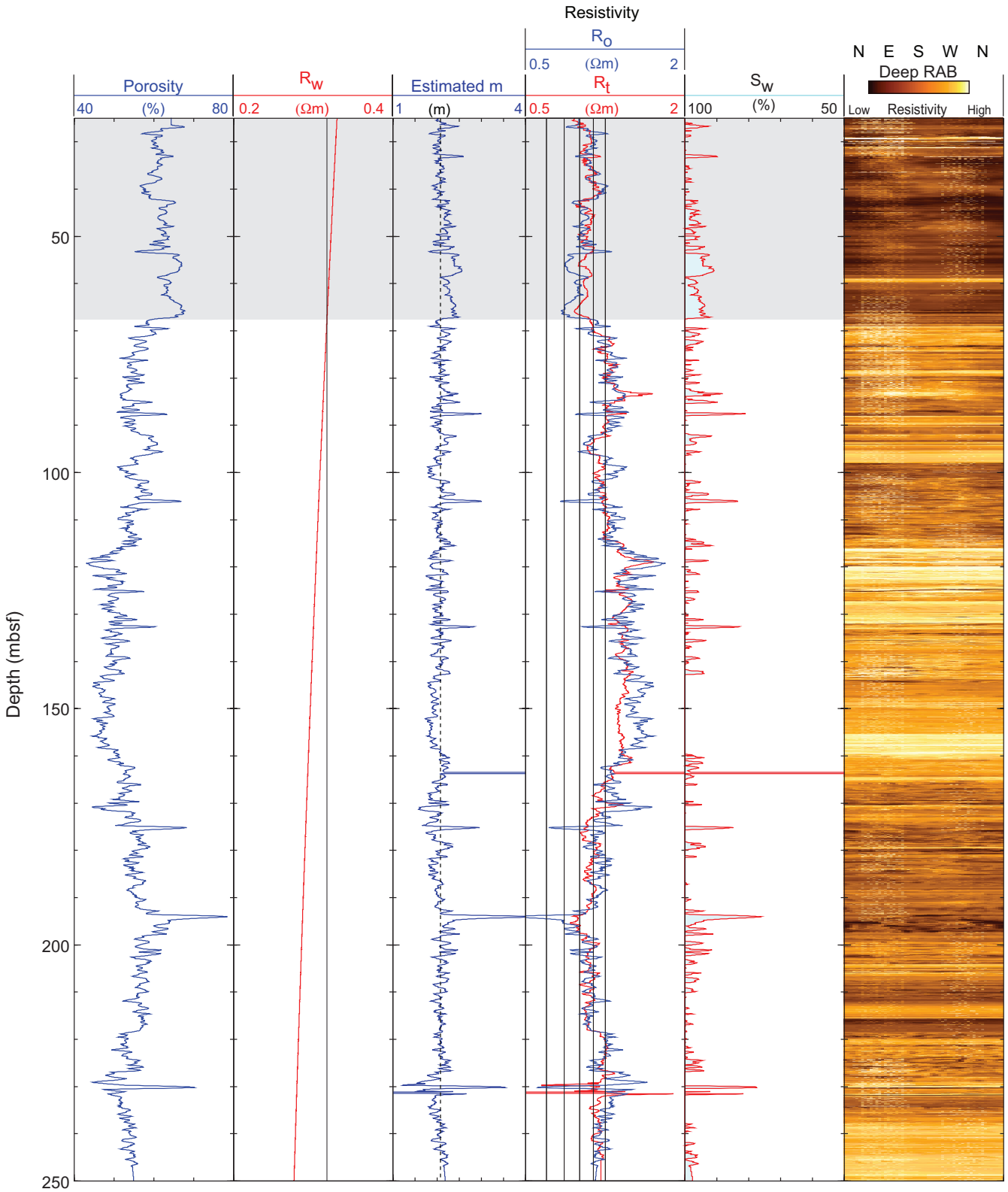

Figure 9. Water saturations from Archie's equation and LWD porosity and resistivity logs in Hole NGHP-01-02B. The gray area indicates degraded data quality. [LWD, logging-while-drilling; R_w, Formation water resistivity; R_0, Computed formation resistivity for 100 percent water saturation; R_t, Measured resistivity; S_w, water saturation]

n=2 (Pearson and others, 1983). We used the "corrected" density porosity computed from the image-derived density (IDRO) and the resistivity from the 16 in, phase-shift, high-frequency propagation resistivity (P16H) measured by the EcoScope tool. We used the P16H curve because it is the resistivity with the highest vertical resolution measured by the EcoScope.

As noted earlier, porosity and resistivity curves in Hole NGHP-01-02B closely mirror each other, so that the computed water-saturated resistivity R_0 is very close to the measured resistivity R_t and the water saturation S_w is close to 100 percent throughout the logged interval (fig. 9). The only exception may be in the shallowest part of the hole, between 20 and 70 mbsf. This is, however, where the hole conditions are the poorest and where the measured bulk densities are least reliable. An enlarged hole will result in an underestimate of density, an overestimate of porosity, and a value of R_0 lower than what it should be. Poor hole conditions, rather than gas hydrates, are the likely explanation of $R_0 < R_t$ above 55 mbsf.

References Cited

Adolph, B., Archer, M., Codazzi, D., el-Halawani, T., Perciot, P., Weller, G., Evans, M., Grant, J., Griffiths, R., Hartman, D., Sirkin, G., Ichikawa, M., Scott, G., Tribe, I., and White, D., 2005, No more waiting—Formation evaluation while drilling: Oilfield Review, Autumn 2005, p. 4–21.

Aldred, W., Cook, J., Bern, P., Carpenter, B., Hutchinson, M., Lovell, J., Rezmer-Cooper, I., and Leder, P.C., 1998, Using downhole annular pressure measurements to improve drilling performance: Oilfield Review, Winter 1998, p. 40–55.

Fofonoff, N.P., 1985, Physical properties of seawater: Journal of Geophysical Research, v. 90, no. C2, p. 3332–3342.

Pearson, C.F., Halleck, P.M., McGuire, P.L., Hermes, R., and Mathews, M., 1983, Natural gas hydrate deposits—A review of *in situ* properties: Journal of Physical Chemistry, v. 87, p. 4180–4185.